c directions. The hydrogen bond parameters are given in Table III.

The main interactions between the *ac* layers are the van der Waals forces among the isobutyl groups of the leucyl side chains that stretch out in the *b* directions. This results in the side chains of dimers from adjacent cells in the *b* direction clustering together inbetween the dimers. This molecular shape with the leucyl side chains at the four corners of the bend regions, stretching out in the *b* direction and the resulting crystal packing, allows the peptide bonds to be easily accessible to the polar solvent molecules and at the same time segregates and clusters together the hydrophobic side chains. Analogous clustering of Phe and Pro side chains to allow formation of water channels is observed for [Phe[4],Val[6]]-antamanide dodecahydrate.[14] The conformation of proteins in aqueous medium is greatly influenced by the entropy factors, and, hence, the folding of the peptide chains are such that the solvent exposure of the hydrophilic groups is maximized with the concomitant minimization of exposure to hydrophobic groups. The folding and packing of the present cyclic peptide molecule are also clearly influenced by such entropy effects.

Comparison with the Conformation in Solution. Superficially, the proton NMR spectra of *cyclo*-(Gly-D-Leu-L-Leu)$_2$ and its close analogue *cyclo*-(Gly-D-Val-L-Leu)$_2$ in dimethyl sulfoxide (Me_2SO) solution are consistent in some aspect with the above conformation of the peptide backbone. However, consideration of the NMR and circular dichroism spectra of these and additional analogues in a range of solvents leads to the conclusion that the dimethyl sulfoxide spectra probably represent an average over two conformations present in comparable amounts. One of these may be the form present in the crystal. In aqueous solutions of water-soluble analogues, such as *cyclo*-(Gly-D-Orn-L-Orn-Gly-D-Val-L-Leu), a single backbone type is clearly indicated, but this is the form with type II L-Yyy-Gly β-turns and extended D-Xxx residues.[2] From the point of view of the short-range intrapeptide interactions, e.g., the calculated conformational energies of the constituent dipeptide units, conformations of this alternative type are as stable as those with type II′ D-Xxx-L-Yyy β-turns. With only small energy differences between alternative backbones, interpeptide interactions will certainly be a deciding factor in the crystal. Such a driving force in the present case is the segregation of polar (peptide bond and water) groups from nonpolar (isobutyl side chains) groups to maximize the polar interactions. It should be noted, however, that here it is still a form of the two β-turn backbone conformation that occurs as in most other cyclic hexapeptides.

Acknowledgment. The diffraction data on GDL were collected at the Protein Institute, Osaka, Japan. Thanks are due to Mr. K. Sakaguchi for technical assistance, Professor M. Kakudo for his hospitality, and the Japanese Ministry of education for the award of visiting professorship to one of us (G. K.). The work was supported by the New York State Department of Health and by the National Institutes of Health, Grant GM-22490.

Supplementary Material Available: Listing of structure factor amplitudes, coordinates of 52 hydrogen atoms included in the structure factor calculation, and the anisotropic thermal parameters (29 pages). Ordering information is given on any current masthead page.

(14) Karle, I. L.; Duesler, E. *Proc. Natl. Acad. Sci.* **1977**, *74*, 2602–2606.

The Nature of the $^1n\pi^* \leftarrow S_0$ Transition. 4.[1] The First Excited Singlet State of Acetaldehyde

Lynn M. Hubbard,[2] David F. Bocian, and Robert R. Birge*

Contribution from the Department of Chemistry, University of California, Riverside, California 92521. *Received August 1, 1980*

Abstract: Medium-resolution electronic-absorption spectroscopy of CH_3CHO and CH_3CDO and laser-induced fluorescence spectroscopy of CH_3CHO are used to study the first excited $^1n\pi^*$ state. A vibrational analysis of the vibronic band system in both absorption and emission gives the following Franck-Condon active $1 \leftarrow 0$ vibrational frequencies for the first excited $^1n\pi^*$ state in CH_3CHO (CH_3CDO): ν_4'[carbonyl stretch] = 1119 cm^{-1} (1173 cm^{-1}); ν_{14}'[out-of-plane bend] = 151 cm^{-1} (112 cm^{-1}); ν_{15}'[methyl torsion] = 187 cm^{-1} (189 cm^{-1}). The system origin (0–0 band) is assigned to the 28 872-cm^{-1} band in CH_3CHO and the 28 975-cm^{-1} band in CH_3CDO. The absorption spectrum of CH_3CHO is characterized by large splittings between the inversion components of ν_{14} in the excited state. The observed out-of-plane bending vibrational levels in the excited state were least-squares fit to the eigenfunctions of a quartic-quadratic potential surface. The optimized surface predicts an equilibrium out-of-plane angle in the excited state of ~26° and a barrier to inversion of ~138 cm^{-1}. We conclude that the barrier to inversion and the out-of-plane angle in the first excited $^1n\pi^*$ state of acetaldehyde are less than their corresponding values in both H_2CO and HCOF. The barrier to rotation of the methyl group in CH_3CHO increases from 400 cm^{-1} in the ground state to ~660 cm^{-1} in the $^1n\pi^*$ excited singlet state. The observed characteristics of the $^1n\pi^*$ state of acetaldehyde are rationalized in terms of significant delocalization of the π^* molecular orbital onto the methyl group.

Although the first excited $n\pi^*$ singlet state of acetaldehyde has been spectroscopically studied in considerable detail,[3-9] no conclusive assignments of the system origin, Franck-Condon active vibrational modes, or the geometry of the excited state are available. As in other aliphatic carbonyl compounds which have been shown to have pyramidal $^1n\pi^*$ states,[10-15] there is spectro-

(1) (a) Parts 1, 2, and 3 of this series are from 1b, 1c, and 1d, respectively. (b) Birge, R. R.; Pringle, W. C.; Leermakers, P. A. *J. Am. Chem. Soc.* **1971**, *93*, 6715. (c) Birge, R. R.; Leermakers, P. A. *Ibid.* **1971**, *93*, 6726. (d) Birge, R. R.; Leermakers, P. A. *Ibid.* **1972**, *94*, 8105.

(2) Department of Chemistry, University of California, Berkeley, CA 94720.

(3) Henri, V.; Schou, S. A. *Z. Phys.* **1928**, *49*, 774.

(4) Leighton, P. A.; Blacet, F. E. *J. Am. Chem. Soc.* **1933**, *55*, 1766.

(5) Eastwood, E.; Snow, C. P. *Proc. R. Soc. London, Ser. A* **1935**, *149A*, 434.

(6) Walsh, A. D. *J. Chem. Soc.* **1953**, 2318.

(7) Rao, V. R.; Rao, I. A. *Indian J. Phys.* **1954**, *28*, 491.

(8) Innes, K. K.; Giddings, L. E., Jr. *J. Mol. Spectrosc.* **1961**, *7*, 435.

(9) Longin, P. *C. Rend. Hebd. Seances Acad. Sci.* **1960**, *251*, 2499.

(10) Brand, J. C. D. *J. Chem. Soc.* **1956**, 858.

(11) Robinson, G. W.; DiGiorgio, V. E. *Can. J. Chem.* **1958**, *36*, 31.

(12) Giddings, L. E., Jr.; Innes, K. K. *J. Mol. Spectrosc.* **1961**, *6*, 528.

(13) Giddings, L. E., Jr.; Innes, K. K. *J. Mol. Spectrosc.* **1962**, *8*, 328.

0002-7863/81/1503-3313$01.25/0

scopic evidence favoring a nonplanar excited $^1n\pi^*$ state for acetaldehyde (with respect to the plane defined by the OCCH skeleton).[8,16] The purpose of this study is to reevaluate the nature of the first excited $^1n\pi^*$ state in acetaldehyde, using vibrational electronic spectroscopy and semiempirical molecular orbital theory.

The previous three papers in this series investigated the nature of the first excited $^1n\pi^*$ states of acrolein and the three singly substituted methyl propenals.[1b-d] The excited state geometry of the $^1n\pi^*$ state in these molecules has at most a three degree out-of-plane angle (relative to the plane defined in the ground state by all atoms disregarding the methyl hydrogens). The $^1n\pi^* \leftarrow S_0$ transition in these molecules, in which the carbonyl group is in resonance with an α-unsaturated group, results from an $\pi^*(\pi) \leftarrow$ n type transition in which the nonbonding electron is promoted into a delocalized π^* molecular orbital.[1c] The essentially planar excited state geometry retains the delocalization of the π electron system. This resonance delocalization is one of two mechanisms which act to stabilize excited $n\pi^*$ states in carbonyl compounds.

An alternate mechanism for stabilization of excited $n\pi^*$ states is hybridization. The promotion of an electron into the π^* molecular orbital results in a partial change in hybridization at the carbonyl carbon from sp^2 to sp^3. This reduces the energy of the π^* orbital, concentrates the π^* electron density primarily on the carbonyl carbon, and results in a change from planar to pyramidal geometry. This mechanism for stabilization was first proposed for formaldehyde by Walsh.[17] Resonance delocalization generally stabilizes $n\pi^*$ states more than hybridization.[1c] Hybridization is primarily responsible for stabilization of the excited $n\pi^*$ state in aliphatic carbonyl compounds, however, where no pathway for resonance delocalization exists.

The first excited $^1n\pi^*$ states of formaldehyde and formyl fluoride (HCOF, isoelectronic with acetaldehyde) have been extensively studied,[10-12,17-19] and a conclusive study of the $^1n\pi^*$ state in acetaldehyde will serve to complete this small family of aliphatic carbonyl compounds. New information can thus be gained concerning substituent effects on the mechanism of stabilization of the $^1n\pi^*$ state. Rao and Rao (1954) were the first investigators to attempt a complete vibrational analysis of the $\pi^* \leftarrow$ n absorption spectrum of acetaldehyde.[7] An excellent discussion of the literature prior to 1954 may be found in their paper. These authors measured 113 bands between 348.5 and 261.0 nm and assigned the system origin (0–0 band) to the 320.4 nm (31 210 cm^{-1}) band. Their vibrational analysis assigned 6 of the 15 normal modes as Franck–Condon active. Although we disagree with their assignments (see below), their spectroscopic study provides the most complete band-position analysis yet available. Longin (1960) recorded the first fluorescence spectrum of acetaldehyde vapor between 360.0 and 480.0 and observed what appeared to be vibrational structure on top of the electronic continuum.[9] The reported vibronic maxima, however, were not reproduced in the present study.

An investigation of the effect of temperature on the vibronic spectrum of acetaldehyde by Innes and Giddings (1961) demonstrated that Rao and Rao's assignment for the 0–0 band could not be correct.[8] Rao and Rao had assumed the longest wavelength band they observed (at 348.3 nm) originated from the ground electronic state in which the vibrational energy was the zeropoint energy plus 2500 cm^{-1}. Innes and Giddings showed the band at 348.3 nm was relatively insensitive to temperature and therefore could not originate from a hot vibrational mode of the ground state. Innes and Giddings concluded that the origin of the electronic transition was near 348.4 nm (28 700 cm^{-1}), the lowest energy band observed by Rao and Rao. No vibrational assignments were made by Innes and Giddings beyond the confirmation of the 1125-cm^{-1} carbonyl-stretching frequency in the excited $^1n\pi^*$ state originally proposed by Rao and Rao.

We report here the first definitive assignment of the system origin at 346.36 nm (28 872 cm^{-1}) and assignment of three Franck-Condon active modes in the first excited $^1n\pi^*$ state of acetaldehyde. A potential function fit to the out-of-plane motion in the excited state is determined and compared to the corresponding potentials in H_2CO and HCOF. An approximate $^1n\pi^*$ excited state geometry, with an out-of-plane angle of $\sim 26°$, and a barrier to inversion of ~ 138 cm^{-1}, results from an analysis of the potential surface for the excited state out-of-plane motion.

Experimental Section

Acetaldehyde (CH_3CHO) was obtained from Mallinckrodt and purified by bulb-to-bulb distillation. Acetaldehyde-d_1 (98+% CH_3CDO) was obtained from Aldrich Chemical Co. The purity of CH_3CHO after distillation and the reported purity of CH_3CDO were confirmed by NMR. All of the spectra were obtained by using a 10-cm path length quartz cell at sample pressures between 200 and 400 mmHg.

The low resolution absorption spectra were recorded at room temperature on a computer-controlled (HP9830) GCA/McPherson double-beam spectrophotometer. Seven measurements were collected at each wavelength interval, and the final spectrum was obtained by averaging three sets of these data (21 measurements per point). A low-pressure mercury lamp was used to provide wavelength standards for both the absorption and emission spectra. The medium resolution spectrum was recorded photographically on a 3.5-m Ebert spectrograph and the photographic plate optical density was graphically obtained by using a Joyce-Loebl microdensitometer. The wavelength calibration was obtained by recording the spectrum of a low-pressure mercury lamp on the same plate used to photograph the spectrum. The instrumental conditions are give in more detail in the appropriate figure captions.

The laser-induced fluorescence spectrum was recorded at room temperature, using a tunable dye laser excitation spectrometer equipped with a gated photon counting detection system.[20] The detection system consists of a 1P28 photomultiplier tube operated at ambient temperature in a radiofrequency shielded housing, a PAR Model 1121 100 MHz amplifier-discriminator operated in pulse coincidence mode with the laser (pulse rate 30 Hz), a high-speed TTL gate, and a 100-MHz counter. A schematic diagram of the spectrometer is shown in Figure 1. The wavelength of excitation was 330.0 nm and was provided by a frequency-doubled (660.0 → 330.0 nm) Chromatix CMX-4 flashlamp-pumped tunable dye laser. The dye laser produced output energies of 0.2–0.8 mJ per pulse (after doubling) at a nominal line width of 3 cm^{-1}, using rhodamine 640 perchlorate as the laser dye. An average of seven measurements was collected at each wavelength interval and the reported emission spectrum was obtained by averaging two sets of these data.

A single pass of the laser beam through the sample generated fluorescence that was too weak to record on the low-intensity blue edge of the fluorescence spectrum. In order to increase the intensity of the fluorescence signal, a reflecting mirror was placed on each side of the sample with the plane of each mirror perpendicular to the direction of the laser beam. The angle between the two mirror planes was varied so that when the laser beam was directed through a hole in the center of the first mirror, multiple passes of the laser excitation occurred through the sample cell.

Results and Discussion

The low-resolution absorption spectra of CH_3CHO and CH_3CDO recorded between 270 and 350 nm are shown in Figure 2. Approximately 60 vibronic bands are observed in the spectrum of each isotopic species, with the absorption maximum occurring at approximately 290 nm for both molecules. The medium-resolution absorption spectrum of CH_3CHO recorded between 324 and 341 nm is shown in Figure 3. The higher resolution of Figure 3 yields partially resolved rotational fine structure superimposed on the individual vibronic bands. The overlapping regions of the absorption and laser-induced fluorescence spectra of CH_3CHO are shown in Figure 4. Fifteen additional bands are observed to the red of the peak at 28 713 cm^{-1} (Figure 4), the longest wavelength band which has been previously reported in the acetaldehyde absorption spectrum.[7]

A. Assignment of the 0–0 Band. The $^1n\pi^* \leftarrow S_0$ transition in acetaldehyde is electric dipole allowed and the 0–0 band should be observable. The system origin is expected to be weak, however, because of the significant change in geometry which occurs upon

(14) Howard-Lock, H. E.; King, G. W. *J. Mol. Spectrosc.* **1970**, *36*, 53.
(15) Judge, R. H.; King, G. W. *J. Mol. Spectrosc.* **1979**, *78*, 51.
(16) Birge, R. R. *J. Am. Chem. Soc.* **1973**, *95*, 8241.
(17) Walsh, A. D. *J. Chem. Soc.* **1953**, 2306.
(18) Jones, V. T.; Coon, J. B. *J. Mol. Spectrosc.* **1969**, *31*, 137.
(19) Fischer, G. *J. Mol. Spectrosc.* **1969**, *29*, 37.
(20) Birge, R. R.; Bennett, J. A.; Pierce, B. M.; Thomas, T. M. *J. Am. Chem. Soc.* **1978**, *100*, 1533.

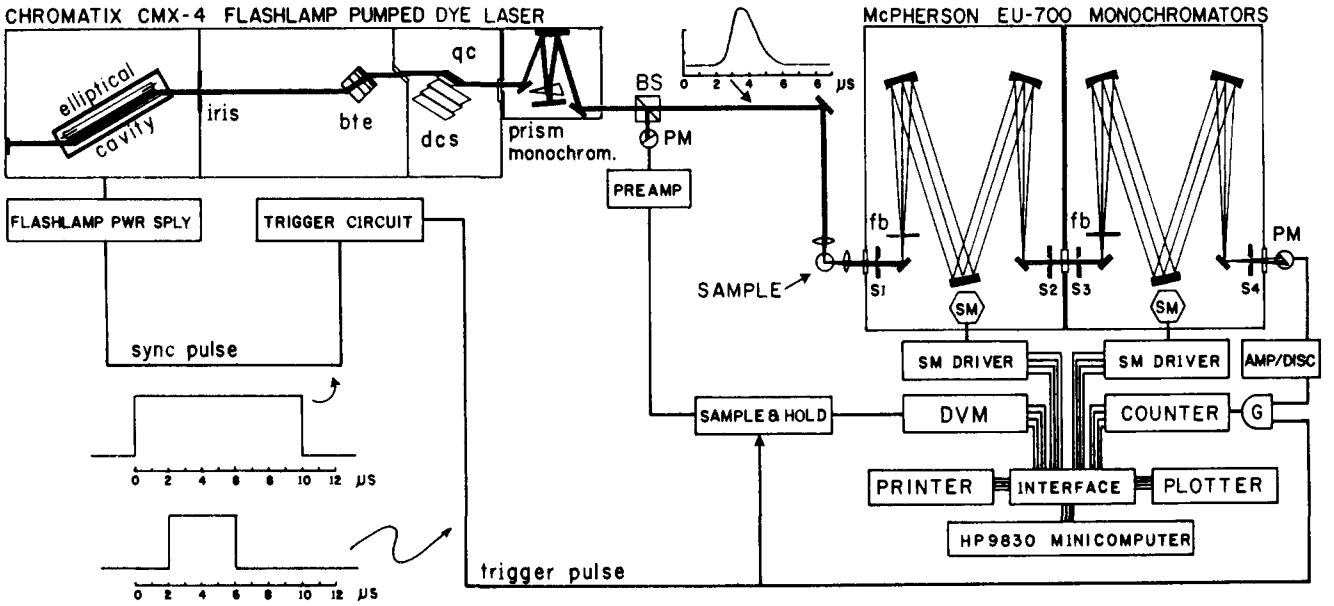

Figure 1. Tunable dye laser fluorescence spectrometer. The emission spectrum shown in Figure 4 was recorded with the fieldstop baffles (fb) removed, the doubling crystal (dcs) in place, and the prism monochromator set at the second harmonic. The other abbreviations denote the following spectrometer components: BS, beam splitter; PM, photomultiplier tube; SM, stepping motor; G, high-speed TTL gate; bte, birefringent tuning element; qc, quartz crystal.

Table I. Observed Ground State (S_0) and First Excited Singlet State [$S_1(^1n\pi^*)$] Vibrational Levels of Acetaldehyde and Acetaldehyde-d_1 (CH_3CDO) (cm^{-1})

			CH_3CHO		CH_3CDO	
assignment	ν_n(mode)[a]	$\Delta\nu$	S_0	S_1	S_0	S_1
C=O stretch	ν_4(a')	1 ← 0	1742	1119	(1743)[b]	1173
		2 ← 1	1736	1098		1151
		3 ← 2		1079		1132
		4 ← 3		1059		1110
		5 ← 4		1032		1094
out-of-plane deformation	ν_{14}(a'')	1 ← 0	764	151	676	112
		2 ← 1	742	322	651	273
		3 ← 2	723	378	641	310
		4 ← 3	716	422	620	357
		5 ← 4	686	468	602	388
methyl torsion	ν_{15}(a'')	1 ← 0	140[c]	187[c]	142[c]	189[c]
		"2" ← "1"	112[d]	170[e]	110[d]	166[e]
		"3" ← "2" app levels[d-k]	13[f]	135[g]	14[f]	138[g]
		"4" ← "3" app levels[d-k]	79[h]	28[i]	82[h]	25[i]
		"5" ← "4" app levels[d-k]		56[j]		66[j]

[a] Mode refers to ground state vibrations only. [b] From ref 22. [c] Assigned to the (1A,1E) ← (0E,0A) transition.[k] The 1A and 1E levels and the 0E and 0A levels are both degenerate to within the experimental uncertainty of our vibronic analysis. [d] Assigned to the 2A ← (1A,1E) transition.[k] [e] Assigned to the (2E,2A) ← (1A,1E) transition.[k] The 2E and 2A levels are degenerate to within the experimental uncertainty of our vibronic analysis. [f] Assigned to the 2E ← 2A transition.[k] [g] Assigned to the 3E ← (2E,2A) transition.[k] [h] Assigned to the 3E ← 2E transition.[k] [i] Assigned to the 3A ← 3E transition.[k] [j] Assigned to the 4A ← 3A transition.[k] [k] See Table V.

excitation (Franck-Condon effects).[1b] Comparison of the absorption and emission spectra of CH_3CHO shown in Figure 4 reveals that there are eight bands which are coincident in the two spectra (to within experimental error). We assign the weak absorption and emission bands observed at 28 872 cm^{-1} (346.36 nm) to the 0–0 transition in acetaldehyde. This assignment is based on our vibronic analysis of the absorption and emission spectra (see below). The vibrational analysis of the absorption spectrum of CH_3CDO indicates that the system origin of this molecule is at 28 975 cm^{-1} (345.13 nm). The observation of a 103-cm^{-1} blue shift upon deuteration is consistent with similar blue shifts of the system origins which occur upon deuteration of HCOF and H_2CO.[10,12,19]

B. Determination of the Franck-Condon Active Vibrations and Assignment of the Vibronic Spectra. Our analysis of the vibronic spectra (see below) indicates that there are three dominant Franck-Condon active modes: the carbonyl stretch (ν_4), the out-of-plane bend (ν_{14}), and the methyl torsion (ν_{15}). The observed vibrational levels in the ground and excited $^1n\pi^*$ states are given in Table I. The numerical values are obtained by a least-squares fit of the vibrational assignments presented in Tables II–IV Near degeneracies in some of the low-lying levels of the methyl torsion vibration were not resolved, hence the use of the term "apparent levels" in Table I (see discussion below). Vibrational assignments of the absorption and emission spectra of CH_3CHO are given in Tables II and III, respectively. Vibrational assignments of the absorption spectrum of CH_3CDO are given in Table IV. Only those vibronic bands included in the least-squares fit are listed in Tables II–IV.

The ground state vibrational frequencies of CH_3CHO and CH_3CDO are well-known from microwave,[21] infrared,[22] and far-infrared[23] studies. The only vibrational frequency for the $^1n\pi^*$

(21) Bander, A.; Günthard, Hs. H. *J. Mol. Spectrosc.* **1976**, *60*, 290.
(22) Hollenstein, H.; Günthard, Hs. H. *Spectrochim. Acta, Part A* **1971**, *27A*, 2027.
(23) Winther, F.; Hummel, D. O. *Spectrochim Acta, Part A* **1969**, *25A*, 417.
(24) Hubbard, L. M. Ph. D. Thesis, University of California, Riverside, 1980.

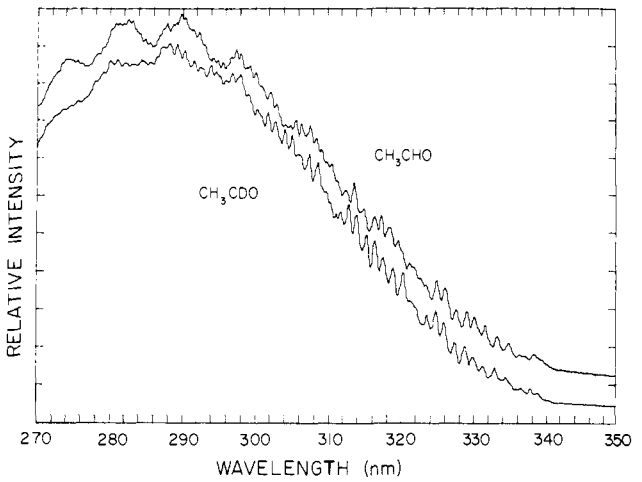

Figure 2. The low-resolution absorption spectra of CH_3CHO and CH_3CDO between 270 and 350 nm. Both spectra represent the average of three different scans in which an average of seven data points were collected per 0.1-nm wavelength interval. The spectrum of CH_3CHO (sample pressure 350 mmHg) was recorded with a spectral resolution of 0.28 nm ($\sim$31 cm^{-1}), using a medium-pressure Hg–Xenon lamp. The spectrum of CH_3CDO (sample pressure 350 mmHg) was recorded with a spectral resolution of 0.23 nm ($\sim$26 cm^{-1}), using a Deuterium lamp. The spectrum of CH_3CDO is shifted below that of CH_3CHO for visual comparison.

excited state previously known with any certainty is the carbonyl stretch, ν_4' (a single prime refers to excited electronic state frequencies and a double prime refers to ground electronic state frequencies). A strong, harmonic progression due to ν_4' with a frequency of $\sim$1125 cm^{-1} has been assigned in the absorption spectrum of CH_3CHO by previous investigators.[7,8] Our assignment of ν_4' (1 $\leftarrow$ 0) is 1119 cm^{-1}, which is consistent with the previous assignment.

1. The Carbonyl-Stretching Vibration. The carbonyl-stretching frequency of CH_3CHO decreases from 1743 cm^{-1} in the ground state to 1119 cm^{-1} in the excited state. The significant decrease in the frequency of this mode indicates that the force constant associated with the carbonyl bond has decreased upon excitation with a concomitant increase in the carbonyl bond length. Simple force constant relationships[1c] predict that the carbonyl bond length increases $\sim$0.18 Å. However, a large change in the normal coordinate description of the carbonyl-stretching vibration is expected between ground and excited states which relegates force constant relationships to only qualitative significance. We conclude on the basis of similarities to H_2CO and HFCO, and our band contour simulations (see below), that the carbonyl bond length increases $\sim$0.11 to $\sim$1.32 Å in the pyramidal excited state.

2. The Methyl Torsion. The observed ground and excited state levels of the methyl torsion are listed in Table I. Some of the low-lying vibrational levels in both the ground and excited $n\pi^*$ states are nearly degenerate and the resolution of our vibronic analysis is insufficient to observe the small splittings. Although our least-squares regression yields differences in the CH_3CHO and CH_3CDO torsional levels, these differences are small and may be due solely to experimental uncertainty.

The observed ground state levels agree well with the detailed experimental and theoretical analysis presented in ref 21 (Table V). The threefold barrier to methyl torsion in the ground state has been calculated to be 400 cm^{-1} (a small negative sixfold potential of -11 cm^{-1} is also present).[21] The considerable Franck-Condon activity of the excited state methyl torsion provides a sufficient number of observed overtones of ν_{15}' to permit the calculation of the threefold barrier to methyl torsion in the $n\pi^*$ excited state. We fit the experimental data to a threefold potential and calculated a barrier height (V_3) of 660 cm^{-1} (Table V). (We did not consider our data to be sufficiently accurate to warrant the inclusion of a sixfold term). We attribute the significant increase in the threefold barrier to methyl torsion upon excitation [$V_3(S_0)$ = 400 cm^{-1}; $V_3(n\pi^*) \simeq$ 660 cm^{-1}] to delocalization of the π^* molecular orbital onto the methyl group. INDO-AFAOS molecular orbital calculations[16] predicts that a majority of the delocalized electron density is placed on the hydrogen atom which is aligned with the $p_z(\pi^*)$ orbital on the carbonyl carbon atom. The increased torsional barrier in the excited state is probably associated with the torsional dependence of the efficiency of delocalization of the π^* electron. INDO-AFAOS calculations correctly predict an increase in the threefold barrier to methyl torsion [$V_3^{calcd}(S_0)$ = 212 cm^{-1}; $V_3^{calcd}(n\pi^*)$ = 279 cm^{-1}], although the absolute magnitudes are seriously underestimated.

3. The Out-of-Plane Deformation. The out-of-plane bending mode (ν_{14}) is the most Franck-Condon active vibration in the absorption (Table II) and fluorescence (Table III) spectra of acetaldehyde. As can be seen by reference to Table I, the observed excited state level splittings in ν_{14}' increase with increasing vibrational quantum number. The divergence of the vibrational energy levels which are high in the potential well is characteristic of a pure quartic oscillator. However, the lower levels are strongly perturbed from pure quartic behavior. This observation is a common feature of a double-minimum potential surface and provides strong evidence in itself for a nonplar $n\pi^*$ excited state.

In order to gain a more quantitative picture of the excited state potential surface, a simple quartic-quadratic potential function was used to simulate the excited state potential surface. The potential function was iteratively modified until the vibrational eigenfunctions matched (using a least-squares criterion) to the observed levels listed in Table I. The accuracy of this approach, however, is limited by the necessity to make certain assumptions

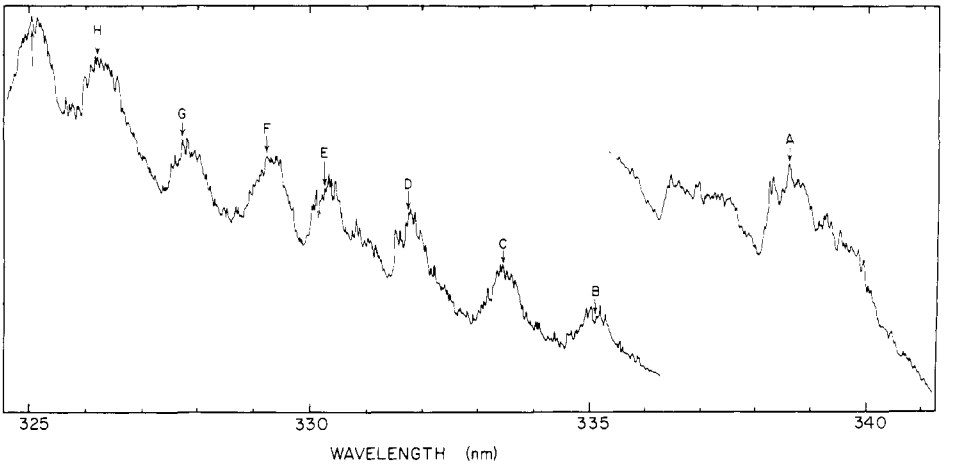

Figure 3. The medium-resolution absorption spectrum of CH_3CHO recorded between 325 and 341 nm. The spectrum was obtained photographically on a 3.5-m Ebert spectrograph, using a high-pressure xenon lamp and translated with a Joyce-Loebl microdensitometer. The spectral resolution is 0.01 nm ($\sim$1 cm^{-1}). The sample pressure was 200 mmHg for the portion of the spectrum recorded between 325 and 336 nm and 400 mmHg for the remainder of the spectrum. The labeled bands correspond to the band labels listed in Table II.

Table II. Vibrational Assignments in the 346.4-nm Absorption System of Acetaldehyde

$\bar{\nu}$,[a] cm^{-1}	Δ_{00}, cm^{-1}	rel int[b]	(ν_4) v', v''	(ν_{14}) v', v''	(ν_{15}) v', v''	error,[c] cm^{-1}	$\bar{\nu}$,[a] cm^{-1}	Δ_{00}, cm^{-1}	rel int[b]	(ν_4) v', v''	(ν_{14}) v', v''	(ν_{15}) v', v''	error,[c] cm^{-1}
27 491	−1381	vw	0, 0	2, 2	0, 4	4	29 987 (C)	1115	m	1, 0	0, 0	0, 0	4
27 582	−1290	vw	0, 0	0, 2	2, 1	1	30 139 (D)	1267	m	1, 0	1, 0	0, 0	3
27 606	−1266	vw	0, 0	0, 2	3, 2	0	30 266 (E)	1394	m	0, 0	5, 0	0, 4	3
27 695	−1177	vw	0, 0	0, 2	5, 2	−5	30 358 (F)	1486	m	1, 0	1, 0	2, 1	1
27 809	−1063	vw	0, 0	0, 2	5, 1	−7	30 497 (G)	1625	m	1, 0	1, 0	2, 0	2
27 840	−1032	vw	0, 0	0, 1	0, 3	3	30 647 (H)	1775	s	1, 0	2, 0	1, 0	4
27 942	−930	w	0, 0	0, 2	5, 0	0	30 750 (I)	1878	s	2, 0	0, 0	0, 4	−5
27 977	−895	vw	0, 0	0, 1	0, 1	−9	30 893	2021	m	1, 0	3, 0	1, 1	−4
28 087	−785	vw	0, 0	1, 2	5, 0	6	31 114	2242	m	0, 0	5, 0	3, 0	−9
28 112	−760	vw	0, 0	0, 1	0, 0	−4	31 270	2398	s	1, 0	4, 0	0, 0	−6
28 191	−681	w	0, 0	1, 1	1, 2	3	31 397	2525	s	2, 0	1, 0	3, 4	−9
28 306	−566	w	0, 0	1, 1	1, 1	0	31 496	2624	s	1, 0	4, 0	3, 3	−5
28 332	−540	vw	0, 0	0, 1	3, 3	3	31 586	2714	s	2, 0	0, 0	3, 0	−5
28 422	−450	w	0, 0	0, 1	5, 3	−3	31 736	2864	m	1, 0	5, 0	0, 0	−4
28 614	−258	w	0, 0	0, 0	0, 2	6	31 867	2995	s	2, 0	3, 0	1, 2	8
28 713	−159	vw	0, 0	0, 0	1, 4	2	31 990	3118	m	2, 0	3, 0	1, 1	−3
28 732	−140	m	0, 0	0, 0	0, 1	0	32 185	3313	m	3, 0	1, 0	0, 1	−6
28 746	−126	vw	0, 0	1, 1	3, 0	5	32 331	3459	w	3, 0	1, 0	2, 4	1
28 769	−103	vw	0, 0	1, 0	0, 2	2	32 404	3532	m	2, 0	4, 0	1, 1	5
28 792	−80	vw	0, 0	0, 0	1, 3	2	32 489	3617	s	3, 0	0, 0	5, 2	3
28 872	0	m	0, 0	0, 0	0, 0	0	32 616	3744	s	2, 0	4, 0	4, 3	1
28 888	16	m	0, 0	1, 0	0, 1	−5	32 701	3829	m	3, 0	1, 0	4, 1	−2
29 033	161	m	0, 0	1, 0	2, 4	3	32 787	3915	w	3, 0	2, 0	3, 4	2
29 056	184	m	0, 0	0, 0	1, 0	3	32 852	3980	m	2, 0	4, 0	3, 0	2
29 083	211	vw	0, 0	0, 0	2, 1	6	32 992	4120	m	3, 0	2, 0	3, 1	1
29 144	272	w	0, 0	0, 0	4, 2	−4	33 080	4208	m	4, 0	0, 0	0, 1	7
29 195	323	vw	0, 0	0, 0	5, 2	1	33 300	4428	m	3, 0	4, 0	0, 1	1
29 212	340	m	0, 0	1, 0	1, 0	−2	33 400	4528	m	2, 0	5, 0	5, 0	6
29 356	484	w	0, 0	0, 0	3, 0	8	33 535	4663	w	3, 0	3, 0	4, 0	4
29 450	578	w	0, 0	0, 0	5, 0	−2	33 602	4730	m	4, 0	1, 0	2, 1	−7
29 474	602	w	0, 0	3, 0	0, 2	−3	34 200	5328	s	5, 0	0, 0	1, 2	−6
29 533 (A)	661	m	0, 0	2, 0	1, 0	−1	34 495	5623	s	4, 0	4, 0	0, 0	5
29 561	689	w	0, 0	2, 0	2, 1	1	34 722	5850	m	4, 0	4, 0	2, 1	−5
29 649	777	w	0, 0	3, 0	1, 3	−4	35 311	6439	s	5, 0	2, 0	5, 0	−3
29 660	788	w	0, 0	3, 0	1, 2	−2	35 386	6514	s	5, 0	4, 0	0, 1	6
29 674	802	w	0, 0	2, 0	5, 2	−5	35 461	6589	s	4, 0	5, 0	3, 0	−1
29 705	833	w	0, 0	2, 0	2, 0	−3	35 537	6665	s	5, 0	4, 0	0, 0	−5
29 719	847	w	0, 0	3, 0	0, 0	4	35 600	6728	s	5, 0	3, 0	3, 0	2
29 833	961	w	0, 0	2, 0	3, 0	4	36 430	7558	s	5, 0	5, 0	5, 1	6
29 847 (B)	975	m	1, 0	0, 0	0, 1	4							

[a] The letters shown in parentheses reference vibronic bands shown in Figure 3. [b] Relative intensity above continuum (vw < w < m < s). [c] Error in the calculated value of Δ_{00} defined as Δ_{00}(calcd) − Δ_{00}(obsd).

concerning the reduced mass of the out-of-plane bending motion as discussed below.

We calculated the reduced mass for the out-of-plane bending vibration under the assumption that the normal coordinate in the excited electronic state is the same as that for the motion in the ground state, since we do not know the exact form of the normal coordinate for the out-of-plane bending motion in the excited state. The form of this coordinate has been determined from normal-coordinate calculations on CH_3CHO.[22] The reduced mass for the vibration was evaluated by the method of Wilson[25] at an equilibrium out-of-plane angle of 30°. The reduced mass was calculated for various equilibrium out-of-plane angles and different forms of the normal coordinate. The calculated changes in the vibrational levels as a function of these slightly different values of the reduced mass were much smaller than the errors associated with the measurement of the positions of the vibronic bands.

The functional form of the potential well was determined by a least-squares fit to a polynomial of the form $V(\theta) = a\theta^4 - b\theta^2$, where a and b are the regression coefficients. Potential functions of this general form have been used extensively to describe the puckering motion in four- and five-membered ring molecules.[26] A slightly different potential function was used by Jones and Coon[18] to calculate the energy eigenvalues for the out-of-plane bending vibration in H_2CO. In our refinements of the potential function, the quartic-quadratic form was maintained and only the constants a and b were varied. The energy eigenvalues for the potential function were obtained from the Tables of Laane.[27] The refined potential function which yields energy eigenvalues giving the best fit to the spectral data is one in which the equilibrium out-of-plane angle in both CH_3CHO and CH_3CDO is ~26° and the barrier to inversion of the two molecules is ~130 cm^{-1}. The potential function for CH_3CHO is shown in Figure 5, and the calculated and observed vibrational frequencies for both isotopic species are compared in Table VI. The good agreement between the calculated and observed ν_{14}' energy levels indicates that a quartic-quadratic potential surface represents a reasonable approximation to the true surface. The out-of-plane angle in the $n\pi^*$ state of CH_3CHO (~26°) is smaller than the out-of-plane angles observed in the $n\pi^*$ states of H_2CO (33.6°)[18] and HFCO (30–35°).[19] Similarly, the barrier to inversion in the $^1n\pi^*$ state of CH_3CHO (~130 cm^{-1})[18] is smaller than those observed in H_2CO (356.2 cm^{-1})[18] and HFCO (2800–4800 cm^{-1}).[19] We tentatively attribute the above differences between CH_3CHO and the other two aldehydes to stabilization of the π^* electron by the methyl group and the calculated (INDO-AFAOS) prediction that the degree of stabilization is enhanced at smaller out-of-plane angles in CH_3CHO.

C. Simulation of the Rovibronic Band Contours. The vibronic bands in the medium-resolution absorption spectrum of CH_3CHO

(25) Wilson, E. B.; Jr.; Decius, J. C.; Cross, P. C. "Molecular Vibrations"; McGraw-Hill: New York, 1955; pp 54–76.

(26) Blackwell, C. S.; Lord, R. C. "Vibrational Spectra and Structure", Durig, J. R.; Ed.; Marcel Decker: New York, 1972; vol. 1, pp 1–24.

(27) Laane, *J. Appl. Spectrosc. (Engl. Transl.)* **1970**, *24*, 73.

Table III. Vibrational Assignments in the 346.4-nm Fluorescence System of Acetaldehyde

$\bar{\nu}$, cm^{-1}	Δ_{00}, cm^{-1}	(ν_4) v', v''	(ν_{14}) v', v''	(ν_{15}) v', v''	error,[a] cm^{-1}
24 504	−4368	0, 1	0, 3	0, 5	−6
24 688	−4184	0, 1	0, 3	1, 5	−3
24 817	−4055	0, 2	0, 1	1, 0	0
24 975	−3897	0, 0	0, 5	0, 3	1
25 129	−3743	0, 2	0, 0	0, 3	0
25 253	−3619	0, 2	0, 0	0, 1	1
25 445	−3427	0, 2	0, 0	1, 1	−4
25 471	−3401	0, 1	0, 2	1, 4	−4
25 510	−3362	0, 0	0, 5	4, 2	−1
25 608	−3264	0, 2	0, 0	2, 1	3
25 787	−3085	0, 0	0, 4	0, 1	0
25 893	−2979	0, 1	0, 2	4, 2	−1
26 062	−2810	0, 1	0, 2	5, 1	−2
26 222	−2650	0, 1	0, 1	0, 1	4
26 415	−2457	0, 1	0, 1	1, 1	−2
26 550	−2322	0, 1	0, 1	1, 0	3
26 695	−2177	0, 0	0, 3	1, 1	−5
26 846	−2026	0, 0	0, 3	2, 1	14
26 987	−1885	0, 1	0, 0	0, 1	3
27 130	−1742	0, 1	0, 0	0, 0	0
27 159	−1713	0, 0	0, 2	1, 5	−9
27 189	−1683	0, 1	0, 0	1, 1	−12
27 241	−1631	0, 1	0, 0	2, 2	−6
27 307	−1565	0, 1	0, 0	1, 0	10
27 360	−1512	0, 0	0, 2	0, 0	6
27 450	−1422	0, 0	0, 2	2, 3	8
27 480	−1392	0, 1	0, 0	3, 1	2
27 525	−1347	0, 0	0, 2	3, 4	−11
27 640	−1232	0, 1	0, 0	4, 0	10
27 778	−1094	0, 0	0, 1	0, 4	−14
27 902	−970	0, 0	0, 1	1, 5	−10
27 949	−923	0, 0	0, 1	1, 4	2
28 098	−774	0, 0	0, 1	0, 0	10
28 345	−527	0, 0	0, 1	3, 2	3
28 425	−447	0, 0	0, 1	5, 3	−6
28 596	−276	0, 0	0, 1	3, 0	4
28 686	−186	0, 0	0, 1	5, 0	−2
28 736	−136	0, 0	0, 0	0, 1	−4
28 877[b]	5	0, 0	0, 0	0, 0	−5
29 019	147	0, 0	0, 0	3, 4	1
29 053	181	0, 0	0, 0	1, 0	6
29 087	215	0, 0	0, 0	2, 1	2
29 146	274	0, 0	0, 0	4, 2	−6
29 197	325	0, 0	0, 0	5, 2	−1

[a] See footnote *c* of Table II. [b] Experimental error is responsible for the 5 cm^{-1} discrepancy between the band maximum observed in the absorption spectrum and in the emission spectrum.

shown in Figure 3 exhibit well-defined contours and some resolved rotational fine structure. We simulated rovibronic band envelopes for the $^1n\pi^* \leftarrow S_0$ transition for various excited state geometries to determine whether the observed band contours are consistent with a pyramidal excited state geometry, which is predicted from our assignments of the first five levels of the out-of-plane bending vibration in the excited state. These excited state geometries were generated by varying the carbonyl bond length, out-of-plane bending angle, CCH angle, and CCO angle. The remaining bond lengths were held fixed at their values in the ground electronic state. The band envelopes were simulated with an asymmetric rotor vibronic band contour computer program developed by Parkin.[28] The maximum values of the limiting symmetric rotor quantum numbers which were included in the simulations were J_{max} equal to 40 and K_{max} equal to 30.

The calculated band contour which best reproduces the observed contours is predominantly type C in character as would be expected for a "perpendicular" $^1n\pi^* \leftarrow S_0$ transition. However, a substantial amount of type A and B character must be included in the contour in order to obtain a reasonable fit to the observed spectra (~20% A, ~20% B). This finding is consistent with

Table IV. Vibrational Assignments in the 345.1-nm Absorption System of Acetaldehyde-d_1 (CH_3CDO)

$\bar{\nu}$, cm^{-1}	Δ_{00}, cm^{-1}	rel int[a]	(ν_4) v', v''	(ν_{14}) v', v''	(ν_{15}) v', v''	error,[b] cm^{-1}
27 902	−1073	vw	0, 0	0, 2	4, 3	−2
28 021	−954	vw	0, 0	0, 2	4, 1	3
28 036	−939	vw	0, 0	0, 1	0, 3	−3
28 144	−831	vw	0, 0	1, 1	0, 3	1
28 255	−720	vw	0, 0	1, 2	3, 0	−2
28 345	−630	vw	0, 0	0, 1	1, 1	1
28 387	−588	vw	0, 0	0, 1	2, 3	1
28 445	−530	vw	0, 0	0, 1	3, 4	−1
28 513	−462	vw	0, 0	0, 1	2, 1	−1
28 536	−439	vw	0, 0	0, 1	3, 2	4
28 713	−262	vw	0, 0	0, 0	0, 3	−4
28 828	−147	vw	0, 0	0, 0	0, 1	5
28 912	−63	vw	0, 0	0, 0	1, 2	0
28 975	0	vw	0, 0	0, 0	0, 0	0
29 009	34	vw	0, 0	1, 0	1, 3	1
29 090	115	vw	0, 0	1, 0	0, 0	−3
29 165	190	vw	0, 0	0, 0	1, 0	−1
29 212	237	vw	0, 0	0, 0	3, 2	4
29 499	524	vw	0, 0	0, 0	4, 0	−6
29 577	602	w	0, 0	1, 0	3, 0	3
29 691	716	w	0, 0	2, 0	5, 2	1
29 886	911	w	0, 0	4, 0	0, 1	−1
30 021	1046	m	0, 0	4, 0	0, 0	6
30 166	1191	w	0, 0	3, 0	3, 0	−3
30 285	1310	m	1, 0	2, 0	0, 2	−4
30 395	1420	m	1, 0	2, 0	0, 1	−4
30 525	1550	m	1, 0	2, 0	0, 0	8
30 665	1690	s	1, 0	0, 0	4, 0	1
30 769	1794	s	0, 0	5, 0	2, 0	1
30 883	1908	m	1, 0	2, 0	2, 0	5
31 201	2226	s	1, 0	4, 0	0, 0	−1
31 338	2363	s	1, 0	3, 0	3, 0	−2
31 586	2611	s	1, 0	5, 0	0, 0	2
31 696	2721	s	1, 0	4, 0	3, 0	−3
31 837	2862	s	1, 0	5, 0	4, 3	3
31 949	2974	s	1, 0	5, 0	2, 0	−6
32 062	3087	m	2, 0	2, 0	4, 1	−2
32 268	3293	m	2, 0	2, 0	5, 0	0
32 383	3408	s	3, 0	1, 0	1, 4	1
32 510	3535	s	2, 0	3, 0	4, 0	2
32 626	3651	m	3, 0	0, 0	1, 0	−6
32 755	3780	s	3, 0	2, 0	1, 2	−2
32 873	3898	s	3, 0	3, 0	0, 2	1
33 003	4028	m	3, 0	2, 0	1, 0	2
33 124	4149	m	3, 0	3, 0	0, 0	2
33 289	4314	m	4, 0	0, 0	0, 2	0
33 422	4447	m	3, 0	4, 0	1, 2	−2
33 670	4695	m	3, 0	4, 0	1, 0	2

[a, b] See Footnotes *b* and *c*, respectively, of Table II.

Chandler and Goodman's polarization study of the $\pi^* \leftarrow n$ transition in CH_3CHO, in which it was found that a substantial fraction of the transition moment lies in the plane containing the A and B inertial axes of the molecule.[29]

The exact shape of the rovibronic band envelope is determined by the equilibrium geometry of the molecule in both the initial and final vibrational states of the vibronic transition. We did not attempt to optimize the geometry to reproduce the detailed features of each of the observed bands, but rather to determine a geometry which resulted in a calculated contour which was in qualitative agreement with the general features of several of the bands. [The resolution of our absorption spectrum (Figure 3) is not sufficient to merit a detailed simulation of the rotational structure.] Nevertheless, we found that it is not possible to reproduce the observed contours *even qualitatively* unless the molecule is bent 25–33° out-of-plane in the excited state. This range in deformation angles is in good agreement with the more precise value predicted for the excited state from our analysis of ν_{14}'. (A more precise

(28) Parkin, J. E.; Innes, K. K. *J. Mol. Spectrosc.* **1965**, *16*, 93.

(29) Chandler, W. D.; Goodman, L. *J. Mol. Spectrosc.* **1971**, *37*, 33.

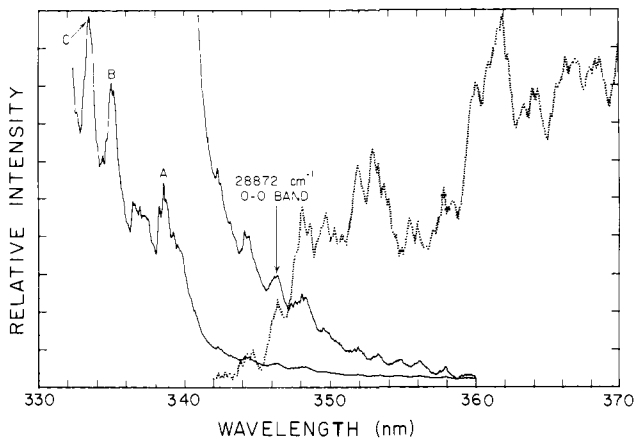

Figure 4. The absorption and emission spectra of CH_3CHO recorded near the system origin (28 872 cm^{-1}). The absorption spectrum (sample pressure 20 mmHg) represents the average of 14 data points collected per 0.04-nm wavelength interval. The spectral resolution is 0.05 nm (~4.4 cm^{-1}). The emission spectrum is not corrected for wavelength dependence of the photomultiplier and monochromator efficiencies and is plotted as the log of the photon count rate. The emission spectrum (sample pressure 350 mmHg) was recorded in 0.1-nm intervals with a spectral resolution of 0.36 nm (~32 cm^{-1}), using a gated photon counting detection system (see Figure 1). The spectrum represents an average of two different scans in which an average of seven data points were collected per wavelength interval. The absorption and emission spectra have been normalized to facilitate the comparison of the coincident bands in the low-intensity edges of the spectra.

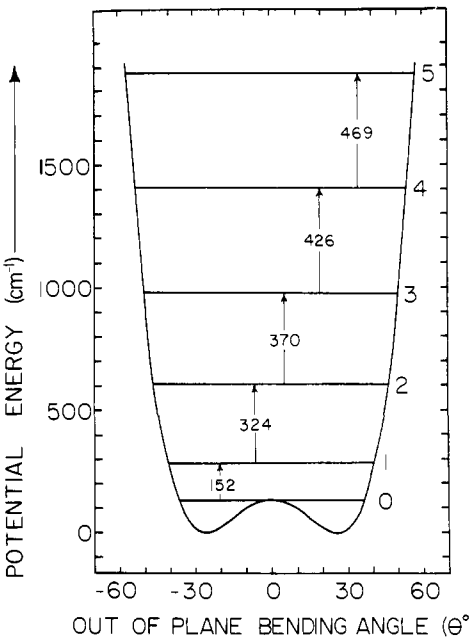

Figure 5. The potential energy well for the out-of-plane bending vibration (ν_{14}') in the first excited $^1n\pi^*$ state of CH_3CHO. The energy levels were calculated from the potential function described in footnotes *a* and *b* of Table VI. The barrier to inversion is 138 cm^{-1} and the minimum-energy out-of-plane angle is 26°.

Table V. Calculated[a,b] and Observed Energy Levels (cm^{-1}) for the Methyl Torsion (ν_{15}) in CH_3CHO and CH_3CDO

mode	level	E^{calcd} *a,b*	Δ_0^{calcd} *a,b*	CH_3CHO Δ_0^{obsd}	CH_3CDO Δ_0^{obsd}
$\nu_{15}''(a'')$	0A,0E	74	0		
	1E	215	141	140	142
	1A	216	142		
	2A	326	252	252	252
	2E	340	266	265	266
	3E	418	344	344	348
	3A	477	403	(403)[c]	
ν_{15}'	0A,0E	100	0		
	1E,1A	290	190	187	189
	2A	457	357	357	355
	2E	460	360		
	3E	591	491	492	493
	3A	616	516	520	518
	4A	678	578	576	584

[a] Calculated ground state levels are taken from ref 21. [b] Excited state methyl torsion levels were calculated to provide the best fit to the observed levels yielding a threefold potential-energy barrier of 660 cm^{-1} assuming $B = 7.32$ cm^{-1} and $V_6 = 0$. [c] Not included in least-squares fit.

value of the out-of-plane angle could not be determined from rotational contour analysis because nearly identical rotational constants can be obtained for this range of out-of-plane angles by varying the other geometrical parameters.)

Summary and Conclusions

(1) The geometry of acetaldehyde in the first excited $n\pi^*$ singlet state is nonplanar with an equilibrium out-of-plane deformation angle of ~26°.

(2) The barrier to inversion in the $^1n\pi^*$ state of acetaldehyde is ~138 cm^{-1}.

(3) The threefold barrier to methyl rotation increases from 400 cm^{-1} in the ground state to ~660 cm^{-1} in the $^1n\pi^*$ excited state.

(4) INDO-AFAOS theory predicts that the π^* molecular orbital is significantly delocalized onto the methyl group in the $^1n\pi^*$ state, and that the energetic stabilization is enhanced by planarity. We attribute this interaction to be responsible for the smaller out-of-plane angle and smaller barrier to inversion in CH_3CHO relative to corresponding values observed for the $^1n\pi^*$ states of H_2CO and HFCO. The energetic stabilization of the π^* orbital in CH_3CHO is also calculated to exhibit a high degree of torsional dependence associated with the dihedral angle between the methyl group hydrogens and the perpendicular (p_z) orbital on the carbonyl carbon. This latter effect is responsible for the large increase in the barrier to rotation of the methyl group upon excitation.

(5) Simulation of the rotational contours of the vibronic bands observed in the absorption spectrum of CH_3CHO indicates that these bands are predominantly type C but with significant contributions of type A and type B rotational character. We attribute this observation to a combination of two factors, the nonplanarity

Table VI. Calculated and Observed Energy Levels (cm^{-1}) for the Excited State Out-of-Plane Bending Mode (ν_{14}') in CH_3CHO and CH_3CDO

	CH_3CHO			CH_3CDO		
v	E^{calcd} *a,b*	Δ_0^{calcd} *a,b*	Δ_0^{obsd}	E^{calcd} *a,c*	Δ_0^{calcd} *a,c*	Δ_0^{obsd}
0 (0^+)	134	0	0	124	0	0
1 (0^-)	286	152	151	239	115	112
2 (1^+)	610	476	473	510	386	385
3 (1^-)	980	846	851	816	692	695
4 (2^+)	1406	1272	1273	1170	1046	1052
5 (2^-)	1875	1741	1741	1562	1438	1440

[a] Calculated using a quartic-quadratic potential function of the form $V(\theta) = a\theta^4 - b\theta^2$. [b] The following regression coefficients and potential surface parameters for CH_3CHO are obtained: $a = 2.96 \times 10^{-4}$ cm^{-1}/deg^4; $b = 4.05 \times 10^{-1}$ cm^{-1}/deg^2; $\theta_{min} = (b/2a)^{1/2} = 26°$; barrier to inversion = $b^2/2a = 138$ cm^{-1}. [c] The following regression coefficients and potential surface parameters for CH_3CDO are obtained: $a = 3.19 \times 10^{-4}$ cm^{-1}/deg^4; $b = 3.99 \times 10^{-1}$ cm^{-1}/deg^2; $\theta_{min} = 25°$; barrier to inversion = 125 cm^{-1}.

of the $n\pi^*$ excited state and the mixing of allowed character into the $\pi^* \leftarrow n$ transition from higher energy transitions polarized in the plane of the molecule.[30]

(6) The carbonyl bond length of CH_3CHO increases ~0.11 Å upon excitation into the $^1n\pi^*$ state.

(30) Pople, J. A.; Sidman, J. W. *J. Chem. Phys.* **1957**, *27*, 1270.

Acknowledgment. This work was supported in part by grants from the National Institutes of Health (R.R.B.), the National Science Foundation (R.R.B.), and the National Center for Atmospheric Research (L.M.H.). L.M.H. gratefully acknowledges a UCAR graduate student fellowship (University Corporation for Atmospheric Research). The authors are grateful to J. A. Bennett for his assistance with the measurement of the laser-induced fluorescence spectrum of acetaldehyde.

Organocobalt Cluster Complexes. 23. Novel Chemistry of (Acylmethylidyne)- and (Aroylmethylidyne)tricobalt Nonacarbonyl Complexes[1,2]

Dietmar Seyferth* and Mara Ozolins Nestle

Contribution from the Department of Chemistry, Massachusetts Institute of Technology, Cambridge, Massachusetts 02139. *Received July 28, 1980*

Abstract: (Acylmethylidyne)- and (aroylmethylidyne)tricobalt nonacarbonyl complexes undergo reduction with molecular hydrogen in refluxing benzene with no added catalyst at atmospheric pressure to produce the respective (α-hydroxyalkylidyne)tricobalt nonacarbonyls and, in some cases, the completely reduced alkylidynetricobalt nonacarbonyls. These tricobalt–carbon cluster-substituted ketones also undergo complete reduction to the corresponding alkylidynetricobalt nonacarbonyl when treated with trifluoroacetic acid in refluxing benzene. (Acylmethylidyne)- and (aroylmethylidyne)tricobalt nonacarbonyl complexes also were found to undergo facile thermal decarbonylation to yield the corresponding (alkylmethylidyne)- and (aroylmethylidyne)tricobalt nonacarbonyl complexes. These unusual reactions were attributed to the uniqueness of the C=O bond in these ketones, and a discussion of possible mechanisms is included. In addition, it was found that in refluxing benzene (α-hydroxyalkylidyne)tricobalt nonacarbonyl complexes revert to the respective ketone complexes.

(Acylmethylidyne)- and (aroylmethylidyne)tricobalt nonacarbonyl complexes, I (Figure 1), are readily accessible by several routes: by the reaction of trichloromethyl ketones, $RC(O)CCl_3$, with dicobalt octacarbonyl[3] and by reaction of (acylium-methylidyne)tricobalt nonacarbonyl reagents, $(OC)_9Co_3CCO^+$,[4,5] with reactive aromatic nucleophiles and with weak organometallic alkylating agents. Such cobalt cluster ketones were important intermediates in our development of the chemistry of organocobalt cluster complexes. Their reduction by triethylsilane, followed by acid hydrolysis (eq 1), provided the corresponding alcohols[6] which

$$RC(=O)CCo_3(CO)_9 \xrightarrow{Et_3SiH} \xrightarrow{\text{concd } H_2SO_4} \xrightarrow{H_2O} RCH(OH)CCo_3(CO)_9 \quad (1)$$

were the precursors of the interesting, highly stabilized cluster carbonium ions, $[RCHCCo_3(CO)_9]^+$.[7] This procedure for $RC(O)CCo_3(CO)_9$ reduction was, however, not applicable to highly hindered systems, e.g., $Me_3CC(O)CCo_3(CO)_9$ and $[(OC)_9Co_3C]_2C{=}O$.

Noteworthy and very intriguing was the fact that the reaction of the cluster ketones with triethylsilane occurred under surprisingly mild conditions. 1:1 Triethylsilane/$RC(O)CCo_3(CO)_9$ reactions carried out in tetrahydrofuran at reflux (~65 °C) under an atmosphere of carbon monoxide for about 8 h gave excellent alcohol yields. As noted in our report of this reaction,[6] silicon hydride addition to ketones generally requires high temperatures, UV irradiation, or transition-metal catalysis. This aspect of the chemistry of the $RC(O)CCo_3(CO)_9$ complexes seemed worthy of closer investigation.

Table I. Reduction of (Acylmethylidyne)- and (Aroylmethylidyne)tricobalt Nonacarbonyl Complexes with Hydrogen

R in $RC(O)CCo_3(CO)_9$	reaction time, h	% yield $RCH_2CCo_3(CO)_9$	% yield $RCH(OH)CCo_3(CO)_9$
H	3	52	0
CH_3	7	8	31
CH_3CH_2	7	4	23
$CH_3CH_2CH_2CH_2$	6	6	26
p-BrC_6H_4	3	0	79
p-ClC_6H_4	3	0	76
p-FC_6H_4	3	0	83
C_6H_5	3	0	78
p-$CH_3C_6H_4$	2	0	83

The chemistry of the Si—H bond of silicon hydrides in many ways closely parallels that of the H—H bond of molecular hydrogen, especially in the case of transition-metal-catalyzed processes. That being the case, it seemed tempting to consider the possibility of the *direct reduction* of our cobalt cluster ketones by molecular hydrogen. Since their C=O bond is so reactive toward the Si—H function of triethylsilane, their reduction by H_2 might proceed under relatively mild conditions.

Our first experiment[2,8] was carried out with (acetylmethylidyne)tricobalt nonacarbonyl. When this cluster ketone

(1) Part 22: Seyferth, D.; Withers, H. P., Jr. *J. Organomet. Chem.* **1980**, *188*, 329.
(2) Preliminary communication: Seyferth, D.; Nestle, M. O.; Eschbach, C. S. *J. Am. Chem. Soc.* **1976**, *98*, 6724.
(3) Seyferth, D.; Hallgren, J. E.; Hung, P. L. K. *J. Organomet. Chem.* **1973**, *50*, 265.
(4) Seyferth, D.; Hallgren, J. E.; Eschbach, C. S. *J. Am. Chem. Soc.* **1974**, *96*, 1730.
(5) Seyferth, D.; Williams, G. H.; Nivert, C. L. *Inorg. Chem.* **1977**, *16*, 758.
(6) Seyferth, D.; Williams, G. H.; Hung, P. L. K.; Hallgren, J. E. *J. Organomet. Chem.* **1974**, *71*, 97.
(7) Seyferth, D.; Williams, G. H.; Eschbach, C. S.; Nestle, M. O.; Merola, J. S.; Hallgren, J. E. *J. Am. Chem. Soc.* **1979**, *101*, 4867.
(8) Eschbach, C. S. Ph.D. Thesis, Massachusetts Institute of Technology, 1975.

0002-7863/81/1503-3320$01.25/0